Adsorption of the Guanine Molecule Over the Pristine, Nb- and Au-doped Boron Nitride Nanosheets: A DFT Study

Meryem Derdare
Universite 8 Mai 1945 Guelma
ABDELGHANI BOUDJAHEM (boudjahem@yahoo.fr)
Computational Catalysis Group, University of GUELMA, Box 41, 24000, Guelma, Algeria

Research Article

Keywords: DFT, Au-doped BN nanosheet, guanine, adsorption, electronic sensitivity

Posted Date: February 23rd, 2021

DOI: https://doi.org/10.21203/rs.3.rs-222751/v1

Abstract

A theoretical study has been performed onto the pristine, Nb- and Au-doped boron nitride (BN) nanosheets using DFT calculations with the B3LYP-D3 method in order to evaluate their stabilities and electronic properties. The interaction of the guanine molecule with these clusters was also examined in aim to determine their adsorption properties. The calculations show that the HOMO-LUMO energy gap (E_g) of the BN nanosheet was strongly decreased upon its doping with Nb and Au atoms, implying a strong enhancement in its surface reactivity. The interaction of the guanine with the BN sheet was found to be weak, which leads a slight variation in its energy gap, therefore a low sensitivity of this nanosheet toward the guanine was observed. The guanine adsorption over the NbBN cluster is very strong, and the calculated adsorptions energies are in the range of – 36.7 to – 60.2 kcal mol^{-1}, suggesting a great chemical adsorption. For the AuBN cluster, the guanine molecule has been chemisorbed onto its surface with adsorption energies varying of – 24.2 to – 38.4 kcal mol^{-1}, which are lower than those obtained for the NbBN cluster. Upon adsorption proceess, the energy gap of the NbBN cluster was greatly increased, which leads to a decrease in its electric conductivity, thereby it cannot be a suitable sensor for the guanine molecule. On the contrary, the energy gap of the AuBN cluster was reduced by the effect of the guanine adsorption on its surface, indicating an increase in its electrical conductivity, thus the AuBN cluster possess a great electronic sensitivity to the guanine molecule. Based on the transition state theory, the recovery time of the guanine from the AuBN cluster was estimated of 27.6 s, reflecting that the Au-doped BN nanosheet could be employed as an appropriate nanomaterial for the guanine molecule detection with a short recovery time.

1. Introduction

Small metal clusters dispersed over different supports have received great deal of interest in heterogeneous catalysis, due to their excellent catalytic properties in comparison with the bulk metal [1–6]. The reactivity of these nanocatalysts is largely influenced by the method of preparation, cluster size, geometry and the metal composition [7–10]. The nature of the support plays also a crucial role in the reactivity of the nanocatalysts [11–12]. For example, in the dehydrogenation of 2-octanol, the rhenium clusters supported on Al_2O_3 are found to be more active than those supported on SnO_2, and the catalytic activity of the particles was multiplied by 5.2 when Al_2O_3 support was replaced by SnO_2 [11]. This difference in reactivity is strongly related to the nature of the interaction (strong or low) between the clusters and the surface of the support. The graphene and its analogous such as boron nitride (BN) sheet are widely employed as an effective support for the metal clusters in order to enhance their catalytic properties in many heterogeneous reactions [12–16]. As an example, Rh nanoparticles dispersed over the surface of the graphene (Rh/Gr) show great catalytic activity in dehydrogenation of ammonia borane as compared to other classical supports such as SiO_2, C and Al_2O_3. The calculated specific activity (TOF) of the Rh/Gr nanocatalyst in the above reaction was found 2 times higher than that found for the Rh/Al_2O_3

one [12]. The BN nanosheet and its analogous were also largely employed as the drug delivery vehicles [17–19]. For example, the BN nanosheet was successfully used for the adsorption of pharmaceutical drugs such as levofloxacin, tetracycline and curcumin [17]. Also, the boron carbonitride nanosheet was found as a suitable vehicle for the paclitaxel drug [18].

BN sheet was considered as a novel structure of B and N atoms which can be employed as an adequate material support for the metal nanoclusters in aim to obtain an efficient nanocatalyst for many chemical reactions such as the oxidation of alcohols, reduction of 4-nitrophenol and hydrogen generation from ammonia borane [14–16, 20]. The reactivity of the nanocatalyst supported on BN sheet in the above reactions has been found to be very high in comparison with that of the classical nanocatalysts. This great catalytic activity of the nanocatalyst was ascribed to the high specific surface area of the BN nanosheet which facilitate the dispersion of the metal clusters over its surface, thereby leads to a better reactivity of the nanocatalyst in these reactions.

The doping of BN sheet by a TM atom is an efficient way to improve significantly its chemical stability, electronic and catalytic properties. The experimental studies show that the reactivity of the BN nanosheet was greatly increased when the metal clusters of small size are dispersed over its large surface [21–24]. For example, the BN sheet which was synthesized in the presence of the ethylene glycol has been found an appropriate support for the Ag, Au and Pt nanoparticles. These nanoparticles supported over the BN sheet are found to be very active in the reduction of p-nitrophenol at mild conditions [23]. The Cu_2O/BN nanocatlyst which was obtained by the dispersion of the Cu_2O particles over the surface of the BN sheet show superior catalytic activity in the reduction of p-nitrophenol to p-aminophenol compared to that obtained for the Cu_2O particles and the pure BN nanosheet [21].

Ni nanoparticles deposited on BN sheet were prepared by reduction of Ni^{2+} by $NaBH_4$ in aqueous medium at room temperature in their catalytic performances were tested in the hydrolysis reaction of ammonia borane [24]. The results show that the obtained Ni nanoparticles are found well dispersed on the surface of the BN sheet and their catalytic activity in the hydrogen production from hydrolysis of ammonia borane was found to be much higher than that obtained for the Ni nanoparticles and the pure BN sheet. Furthermore, the recyclability test demonstrates that the Ni/BN nanocatalyst can retained 83 % of its reactivity after five cycles of hydrolysis reaction.

A high catalytic activity was obtained in Suzuki-Miyaura reaction for the PdFe nanoparticles supported over the surface of the BN sheet [22]. This strong reactivity of these nanocatalysts was attributed to the synergetic effect, which is due to the Pd-Fe core-shell configuration and their interaction with the BN nanosheet. Moreover, when the BN sheet was replaced by the oxide graphene (GO), the results show that the reactivity of the Pd-Fe/GO nanocatalyst was found lower than that of the Pd-Fe/BN nonacatalyst. This finding reflects that the BN sheet employed as support for the metal nanoparticles is a suitable way to obtain a efficient nanocatalyst which is very active in many catalytic reactions.

In the last decade, the theoretical studies were focused onto the properties of the TM-doped of the BN nanosheet, which are extensively employed either as vehicles for the drug delivery or as active nanocatalysts for different catalytic applications. These nanoclusters formed by the doping of the BN nanosheet with TM atoms have also been studied computationally in aim to better understand their electronic sensitivity toward the toxic molecules [25]. For example, Vessaly et al. [25] have studied theoretically the adsorption of SO_2 over the pristine and the Si- and Al-doped BN nancheets using B3LYP/6-31G level of theory, and the obtained results by them indicate that the BN nanosheet which is doped with Al and Si possess a great sensitivity toward SO_2 gas, while the pure BN sheet was found to be insensitive to SO_2, and thereby this molecule cannot be detected by the BN sheet as a toxic gas in a polluted environment. Also, due to its high surface area and its great reactivity which are reported in several experimental studies, the BN nanosheet was effectively employed as a catalyst support in several catalytic reaction mechanisms which takes place on the catalyst surface [26, 27]. Also, the BN nanosheet has been mainly employed as vehicles for the drug delivery in a biological environment [28–30]. As an example, Lin et al. [29] have investigated the interaction of the guanine, adenine, thymine and cytosine and uracil with the pure BN nanosheet. The calculated adsorption energies are in the range of 11.5 to 15.9 kcal mol^{-1}, indicating a physical adsorption. The results exhibit also that the nature of these nucleobases remains unchanged after interaction with BN sheet, which suggest that the BN nanosheet can be considered as a promising nonocarries for these molecules in the biological systems. The adsorption of DNA nucleobases such as guanine and adenine over the BN sheet and graphene has been studied by Lee et al. [28] using DFT (PBE-vdW) calculations. The obtained results reveal that the binding energies range from 21.4 to 27.2 kcal mol^{-1}, reflecting a physisorption process. The reduction of NO over Si-doped BN sheet in the presence of CO molecule was investigated by PBE/DNP level with the empirical dispersion terms [27]. The doping of BN nanosheet with Si atom increases its surface reactivity, thus the Si atom in the cluster can plays a crucial role in the mechanism of the reduction of NO. The formation of the N_2O molecule from $(NO)_2$ dimer over the Si/BN catalyst has been found to be the most likely mechanism for this reaction. The activation barrier for the reduction of NO is of 9.0 kcal mol^{-1}, Moreover, the remaining oxygen atom attached to the surface of the cluster is then removed by its reaction with CO gas to form the desorbed CO_2 gas. This formation of CO_2 molecule from CO requires a little activation energy of about 7.8 kcal mol^{-1}.

In this work, a theoretical study was performed on the pristine, Nb- and Au-doped boron nitride (BN) nanosheets using DFT calculations with the B3LYP-D3 method in order to investigate their stability and electronic properties. The electronic sensitivity of these clusters toward the guanine molecule has also been examined and the obtained results were analyzed and discussed.

2. Theoretical Method

DFT calculations with the B3LYP-D3 method were carried out by the Gaussian09 package [31–34] to evaluate the stability and electronic properties of the pristine, Nb- and Au-doped boron nitride (BN) nanoscheet. The interaction of the guanine molecule with the BN, NbBN and AuBN clusters has also been

investigated with the same method in aim to examine their adsorption properties and electronic sensitivity. The B3LYP hybrid functional with the Grimme's dispersion (D3) correction were often used in the studies of the stabilities, electronic and adsorption properties of the nanomaterials and yielded acceptable results which are well close to the experimental data [35–36]. Meanwhile, the LanL2DZ effective core potential (ECP) basis set was used for the Nb and Au atoms, and the 6-311G(d,p) basis set has been employed for the B, N, O and H atoms [37–38]. These two kinds of basis sets were chosen for their accuracy in which the theoretical values obtained for the studied nanostructured systems are well matched with the experimental results [39–42].

The BN nanosheet employed in our study is containing 23 atoms of boron, 23 atoms of nitrogen and 18 atoms of hydrogen which are attached to the boron or nitrogen atoms at end of the BN cluster. The Nb- and Au-doped BN nanosheets have been constructed through of a substitution of a B atom of the BN nanosheet by an Au or Nb atom in order to improve their surface reactivity.

Fukui function (f^+) was also calculated in order to determine the active sites on the surface of the NbBN and AuBN clusters. The higher values of f^+ correspond to the active sites which may be involved in a chemical reaction. In other words, this function is able to predict the active sites existing on the surface of the studied clusters which can react with the nucleophilic sites of a molecule. So, the Fukui function f^+ for a nucleophilic attack is defined as [43]:

$$f^+(r) = \rho_{N+1}(r) - \rho_N(r) \quad (1)$$

where $\rho_K(r)$ ($K = N$ and $N + 1$) represent the electron density at r in a cluster of a K-electron.

In order to obtain the most stable adsorption configurations, several positions and many orientations of the guanine above the surface of the BN, NbBN and AuBN clusters were optimized. When the guanine molecule was adsorbed onto the surface of the clusters, it is important to know the nature of the interaction between both species by calculating the adsorption energy (E_{ads}) which is given by the following equation.

$$E_{ads} = E_{MBN/guanine} - E_{MBN} - E_{guanine} + E_{BSSE} \quad (2)$$

where E_{MBN} and $E_{MBN/guanine}$ are the total energies of the metal-doped BN nanosheet and the complexes formed through their interaction with the guanine molecule, respectively. E_{BSSE} is the energy of the basis set superposition error.

Similar expression was used to calculate the adsorption energy (E_{ads}) of the guanine adsorption over the surface of the pure BN nanosheet.

$$E_{ads} = E_{BN/guanine} - E_{BN} - E_{guanine} + E_{BSSE} \quad (3)$$

where $E_{BN/guanine}$ is the total energy of the adsorbed guanine on the pure BN nanosheet.

The electronic sensitivity of the BN, NbBN and AuBN clusters to the guanine molecule for a given temperature (T) has also been computed using the Eq. (4). According to the Eq. (4), the energy gap (E_g) of the cluster has been directly related to its electric conductivity (σ). For example, when the E_g of the cluster decreases due to the adsorption of the guanine molecule on its surface, its electrical conductivity rises, which can be converted to an electrical signal. Therefore, the cluster will be a promising candidate to be a good nanosensor for the detection of the guanine molecule.

$$\sigma = A\, T^{3/2} \exp(-E_g / 2\, k\, T) \quad (4)$$

where A is a constant (electrons/m^3 $K^{3/2}$), k is the Boltzman's constant and E_g is the energy gap.

The recovery time of a molecule which is adsorbed over the surface of a cluster is an important criterion for the choice of a nanosensor, The desorption of a molecule which is greatly chemisorbed to the surface of the cluster requires a long recovery time. Thus, the clusters which are strongly attached to the molecules are not appropriate nanomaterials for the nanosensor applications. Experimental study indicates that the recovery of a nanosensor is achieved either by heating to high temperatures or by exposure to UV light. On the basis of the transition state theory, the recovery time of a molecule over the surface of a cluster can be estimated from the Eq. (5), in which we find a direct relationship between the adsorption energy (E_{ads}) and frequency (υ) with the recovery time (τ).

$$\tau = \upsilon^{-1} \exp(-E_{ads} / k\, T) \quad (5)$$

where T, k and υ are the temperature (K), the Boltzman's constant (~ 2.0 10^{-3} kcal $mol^{-1}K^{-1}$) and the attempt frequency (s^{-1}), respectively. E_{ads} is the adsorption energy of the molecule over the surface of the cluster.

3. Results Discussion

3.1 The electronic properties of the pristine and the Nb-, and Au-doped BN nanoscheets

The geometries of the pristine and the Nb-, and Au-doped BN nanosheets were optimized, and the most stable configurations obtained are shown in Fig. 1. The density of states (DOS), molecular electrostatic potential (MEP), energies of HOMO and LUMO states (E_H and E_L), energy gap (E_g), charge on metal atom (q_M), electric dipole moment (β), chemical hardness (η) and the softness (s) have been calculated, and the results predicted are shown in Fig. 2 and Table 1. The calculated length of the B-N bond in the pure BN sheet was found to be 1.45 Å, which is in good agreement with the values reported by the other researchers [44, 45]. When a B atom of BN sheet was replaced by an Au or Nb atom, a small deformation in the geometry of the pure BN nanocage was observed, in which the metal atom was slightly taken out of the surface of the formed cluster after doping. The distance of the newly formed M-N bond in the Au-

and Nb-doped BN clusters are found to be 2.11 and 2.02 Å, respectively, which are larger than that of the value obtained of the B-N bond in the pure BN nanosheet. The binding energy (E_b) of the BN sheet was found to be – 5.431 eV, indicating that this nanosheet has a strong stability. Doping of the BN nanosheet by an Au or Nb atom has slightly decreased its binding energy and the calculated E_b values are – 5.336 eV and – 5.327 eV for the AuBN and NbBN clusters, respectively. Moreover, the values of E_b are found to be very negative, which reflect a great stability of the two clusters upon doping. These results confirm the positive values obtained for the vibrational frequencies for both clusters, in which the calculated values range from 21.5 and 21.9 cm^{-1} to 47.2 and 45.6 cm^{-1} for the NbBN and AuBN clusters, respectively.

Table 1. The interaction distance (d), binding energy (E_b), energies of HOMO and LUMO states (E_H, E_L), energy gap (E_g), charge on metal atom (q_M), dipole moment (β), chemical hardness (η) and softness (s) of the pure and Nb and Au-doped BN nanosheet.

Cluster	d (Å)	E_b (eV/atom)	E_H (eV)	E_L (eV)	E_g (eV)	q_M (e)	β (D)	η* (eV)	s* (eV^{-1})
BN	1.45	-5.431	-6.573	-0.541	6.032	+0.382**	0.217	3.016	0.166
NbBN	2.02	-5.327	-3.540	-2.045	1.495	+1.064	0.936	0.748	0.668
AuBN	2.11	-5.336	-6.313	-3.611	2.701	+0.287	0.938	1.351	0.370

* The chemical hardness was calculated by $E_L - E_H / 2$ and the softness was estimated by 1/2 η.

** Charge on B atom in BN sheet which was substituted by Au or Nb atom.

The energies of the HOMO and LUMO orbitals of the pristine are – 6.573 and – 0.541 eV, respectively, thereby a gap energy of 6.032 eV, suggesting that a semiconductor behavior can be manifest in this nanomaterial despite its large-band gap. Moreover, the estimated value of E_g of BN sheet is in excellent agreement with the experimental values reported in the literature which vary between 3.6 and 7.1 eV [46]. The electronic properties of the BN nanosheet were strongly modified when a B atom was replaced by an Au or Nb atom (see Table 1). For example, the value of E_g was decreased from 6.032 eV in the BN sheet to 1.495 and 2.701 eV in the Nb- and Au-doped BN nanosheets. respectively. So, the variation in E_g (ΔE_g) after substitution of a B atom by a Nb and Au atoms was found to be 75.2 and 55.2 %, respectively, implying a deep alteration in the surface reactivity and electronic properties of the BN nanosheet upon doping. Therefore, the stability of the BN nanosheet has been strongly decreased after its doping with an Au or Nb atom. In other words, the doping with metal atom greatly enhances the reactivity of the pure BN sheet. That is to say, the AuBN and NbBN clusters are found to be more reactive than the BN sheet, thus their interaction with the nucleophilic centers of a molecule is done more easily than the pure BN sheet. This increase in reactivity was confirmed by the values of the chemical hardness (η) and the softness (s) of the BN nanosheet which were calculated before and after metal doping. The values of η were sharply

diminished after metal doping (η decreases from 3.016 in the BN sheet to 0.748 and 1.351 eV in NbBN and AuBN nanoclusters, respectively). In cluster science, the chemical hardness is an important parameter that characterizes the chemical stability of the cluster [47–49]. A large η value indicates a higher stability, while a little η value suggests a higher chemical reactivity. The calculations of the softness indicate a reverse trend compared to the hardness, where the values are increased from 0.166 $(eV)^{-1}$ in BN sheet to 0.370 and 0.668 $(eV)^{-1}$ in AuBN and NbBN clusters, respectively, confirming that the reactivity of the BN nanosheet was sharply enhanced after doping with Au and Nb atoms. Furthermore, these results are in excellent agreement with the obtained values for the energy gap and the chemical hardness.

The AIM charges analysis of the BN nanosheet exhibits a sizable charge of 0.382 |e| was transferred from the bore to the nitrogen atoms in the pure BN nanosheet, implying the existence of a strong ionic interaction between the B atoms and the N atoms in the BN nanosheet. This great interaction between both atoms indicates a high chemical stability of the BN sheet, which is consistent with the calculated values for the binding energy, the chemical hardness and the softness. The direction of the charge transfer in BN sheet has also been confirmed by MEP isosurface (see Fig. 2), where the N atoms are greatly negatively charged (red color), and the B atoms are positively charged (blue color). The Mulliken charge analysis shows also that a large quantity of charge was transferred from metal atom to nearest N atoms in the NbBN and AuBN clusters. The charge predicted over the Nb and Au atoms were found to be + 1.064 and + 0.287 |e|, respectively. The positive charge on Nb and Au atoms in the clusters (blue color) has also been confirmed by MEP analysis (Fig. 2). These results indicate that the Nb and Au atoms in the clusters could be considered as eletrophilic sites, which can easily attacked by the nucleophilic centers of a molecule as the guanine. In order to determine the reactive sites onto the surface of the NbBN and AuBN clusters, the condensed Fukui function (f^+) was calculated, and the results obtained are illustrated in Fig. 3. As it is know, the electrophilic sites existing over the surface of the cluster which are susceptible to be attacked by the nucleophilic sites of a molecule such as the guanine could be described by the high positive value of f^+. In other words, the higher values of f^+ correspond to the most favorable sites in the clusters which are able to react with the nucleophilic centers of the guanine molecule. As it was shown in Fig. 3, the isosurface of f^+ indicates that the highest f^+ values were predicted for the Nb and Au atoms, respectively, suggesting that the two atoms (sites) could be considered as the most favorable adsorption sites over the surface of the clusters, thereby they are susceptible to easily interact with the nucleophilic centers of the guanine. Moreover, the value of f^+ for the Au atom ($f^+ = 0.152$) in the AuBN cluster is lower than that calculated for the Nb atom ($f^+ = 0.397$) in the NbBN cluster, reflecting that the Nb atom in NbBN cluster was found to be more reactive than the Au atom in AuBN cluster. The results show also that the electric dipole moment (β) of the BN nanosheet is slightly increased upon its doping with Nb and Au atoms (see Table 1). It increases from 0.217 D in the pure BN nanosheet to 0.936 and 0.938 D in the NbBN and AuBN nanoclusters, respectively.

3.2 Adsorption of the guanine over the BN nanosheet

In this section, we have studied the reactivity of the BN nanosheet toward the guanine molecule. In order to determine the optimized geometries of the guanine adsorbed over the BN nanosheet, different orientations of the guanine molecule onto the surface of the cluster were tested. Upon optimizations, two stable complexes have been obtained, namely A and B, and their optimized geometries, structural parameters and electronic properties are reported in Fig. 4 and Table 2. The electron density of the HOMO and LUMO orbitals of the two complexes have also been shown in the Fig. 4. As one can see from the Fig. 4, the guanine molecule was adsorbed parallel to the surface of the BN nanosheet in both states. The distance between the guanine molecule and the surface of the BN cluster is 3.27 and 3.36 Å for the A and B configurations, respectively (Table 2). These large interaction distances suggest that the adsorption of the guanine over the surface of the BN sheet is weak, and the calculated adsorption energies (E_{ads}) are − 15.2 and − 14.9 kcal mol^{-1} for the A and B complexes, respectively, indicating a physical adsorption. The interaction of guanine with B_{40} nanocage has been investigated by Cheng et al. [50] by using PBE/DNP method. Upon optimizations, they found five most stable complexes with adsorption energies which vary between – 23.6 and – 36.3 kcal mol^{-1}, which are higher than the values obtained in our study. On the contrary, the computed adsorption energy by Lin et al. [29] for the interaction between the guanine and the h-BN nanosheet (E_{ads} = 15.9 kcal mol^{-1}) was found almost equal to the values predicted in our calculations. The energies of the HOMO and LUMO states, energy gap (E_g), charge transfer (q_{CT}) and the dipole moment (β_T) of the formed clusters upon complexation between the BN nanosheet and the guanine molecule were computed and the values obtained are listed in Table 2. The thermodynamic parameters such as entropy change (ΔS), enthalpy change (ΔH) and Gibbs free-energy change (ΔG) for the complexes were also calculated and the predicted values are summarized in the same table. As it was presented in Table 2, the values of ΔH and ΔG are found to be more negative, implying that the interaction process between both specious to forms the complexes is exothermic and thermodynamically spontaneous. The results show also that the HOMO-LUMO energy gap of the BN nanosheet was slightly influenced by the adsorption of the guanine molecule over its surface, and the variation in E_g (ΔE_g) is of 14.9 % and 13.2 % for the configurations A and B, respectively.

Table 2
The The interaction distance (d), energies of HOMO and LUMO states (E_H, E_L), energy gap (E_g), charge transfer (q_{CT}), dipole moment (β_T), adsorption energy (E_{ads}) and thermodynamic parameters (ΔH, ΔS and ΔG) for the complexes A and B.

Complex	d (Å)	E_H (eV)	E_L (eV)	E_g (eV)	q_{CT} (e)	β_T (D)	E_{ads} kcal mol^{-1}	ΔH kcal mol^{-1}	ΔS cal mol^{-1}	ΔG kcal mol^{-1}
A	3.27	-5.835	-0.700	5.134	-0.001	5.326	-15.2	-19.1	-41.3	-6.8
B	3.36	-5.833	-0.595	5.237	-0.010	5.087	-14.9	-20.0	-39.6	-8.2

The HOMO and LUMO orbitals of the complexes which are formed upon the adsorption of the guanine over the surface of the BN sheet (A and B) were calculated and the obtained results are given in Fig. 4. For

the two configurations A and B, the results clearly indicate that the distribution of HOMO is mostly localized over the guanine molecule, whereas the density of LUMO is principally located on the surface of BN nanosheet. This result suggests that the guanine molecule was strongly interacted with the LUMO level of the cluster. Moreover, the results show that small charges were transferred from the BN cluster to the guanine molecule, reflecting a weak adsorption process (Table 2). The AIM charges analysis shows that the quantity of charge transferred between both species is 0.010 and 0.011 |e| in the A and B complexes, respectively (Table 2).

The EDD isosurfaces for both complexes (A and B) were calculated and the results are presented in Fig. 5. Accordingly to Fig. 5, the electron density accumulation between the surface of the BN nanosheet and the guanine molecule is almost negligible, confirming a weak physical adsorption of the guanine over the surface of the BN nanosheet.

3.3 Adsorption of the guanine molecule over the AuBN nanosheet

To study the reactivity of the Au-doped BN nanosheet, we have examined the interaction of the guanine molecule over its surface. In order to find the most stable configurations of the formed complexes after adsorption process, several initial geometries were fully optimized and analyzed. Before optimizations, the guanine molecule was located above the surface of the AuBN cluster through of their nucleophilic sites (oxygen and nitrogen atoms), where each site of the molecule has a large tendency to attack the electrophilic site (Au atom) of the cluster. The complex where the guanine molecule with an orientation parallel to the surface of the AuBN cluster has also been considered in our calculations. As it was mentioned above, the Au atom represents a catalytic active site on the surface of the AuBN cluster which can easily interact with the nucleophilic sites of the guanine molecule. Upon full optimization, five stable complexes namely, C, D, E, F and G were predicted (Fig. 6), and their electronic and adsorption properties are reported in Table 3. The calculations show that the interaction between the guanine molecule and the Au-doped BN nanosheet is very strong, and the predicted adsorption energies are in the range of – 24.2 to – 38.4 kcal mol^{-1} (Table 3). Moreover, in all the formed complexes, the interaction between both species was carried out without deformation of the guanine molecule, suggesting that the fundamental nature of the guanine molecule remains unchanged after adsorption process. This result is very important, especially for the nanomaterials which could be candidate to be good drug nanocarriers.

Table 3

The Table 2. The interaction distance (d), energies of HOMO and LUMO states (E_H, E_L), energy gap (E_g), charge transfer (q_{CT}), dipole moment (β_T), adsorption energy (E_{ads}), enthalpy change (ΔH), entropy change (ΔS) and Gibbs free-enthalpy change (ΔG) for the formed complexes from the interaction of the guanine molecule with the surface of the clusters.

	d (Å)	E_H (eV)	E_L (eV)	E_g (eV)	q_{CT} (e)	β_T (D)	E_{ads} kcal mol^{-1}	ΔH kcal mol^{-1}	ΔS cal mol^{-1}	ΔG kcal mol^{-1}
AuBN-Complex										
C	2.15	-5.297	-2.870	2.427	+ 0.192	13.941	-32.9	-35.3	-38.0	-24.0
D	2.17	-5.414	-2.951	2.463	+ 0.183	10.070	-33.3	-38.3	-42.8	-25.6
E	2.26	-5.884	-3.520	2.364	+ 0.152	6.839	-24.2	-26.7	-42.4	-14.0
F	2.17	-6.037	-3.569	2.469	+ 0.727	3.201	-38.4	-42.4	-45.8	-28.8
G	2.37	-5.744	-3.325	2.419	+ 0.210	5.664	-25.3	-30.9	-44.9	-17.5
NbBN-Complex										
H	2.39	-3.443	-1.801	1.642	-0.682	15.563	-60.2	-64.2	-38.9	-52.6
I	2.31	-3.383	-1.699	1.684	-0.045	5.812	-57.2	-61.1	-36.5	-50.2
J	2.27	-4.373	-1.669	2.704	-0.181	5.603	-50.5	-63.1	-46.0	-49.4
K	2.34	-4.146	-1.569	2.577	+ 0.025	5.113	-36.7	-40.8	-28.9	-32.2
L	2.55	-4.198	-2.024	2.174	-0.079	4.106	-42.1	-47.1	-34.4	-36.9

In the complex C, the guanine molecule is adsorbed onto the Au atom of the AuBN cluster by the lone electron pairs of the nitrogen atom that belongs to the 5-membered ring of the guanine. The interaction between both species is found to be very strong, and the calculated adsorption energy (E_{ads}) of the guanine adsorption on the surface of cluster is – 32.9 kcal mol^{-1}, indicating a chemisorption process. The newly Au-N bond distance which was formed after interaction between the guanine and the AuBN cluster is of 2.15 Å. For the complex D, the same atom of the nitrogen has also been sharply chemisorbed over the Au atom of the AuBN cluster to form a second stable geometry which is completely different (orientation parallel with respect to the surface of the AuBN cluster) than that obtained for the complex C (see Fig. 6). The length of the Au-N bond which was formed upon adsorption process in complex D is

2.17 Å and the calculated adsorption energy was found to be – 33.3 kcal mol^{-1}, which is slightly higher than the value predicted for the complex C, indicating that this geometry is more stable than that found for the complex C. The guanine adsorption over the surface of the AuBN cluster through its nitrogen of -NH_2 has also been predicted in our optimizations (complex E) and the calculated E_{ads} value (– 24.2 kcal mol^{-1}) is lower in comparison with the values predicted for the above configurations (C and D). The distance of the Au-N bond is 2.26 Å, which is a bit greater than the values estimated for the configurations C and D, respectively. In the complex F, the interaction was carried out between the Au atom of the cluster and the N atom that belongd to the 6-membered ring of the guanine with an adsorption energy of – 38.4 kcal mol^{-1}. The highest E_{ads} value was obtained for this complex in comparison with the values calculated for the other configurations, indicating a very strong chemical adsorption between the N atom of the guanine and the Au atom of the AuBN cluster. The distance of the Au-N bond which was formed in complex F after chemisorption process is only 2.17 Å.

In the complex G, the guanine molecule is chemisorbed with an orientation parallel to the surface of the AuBN cluster. This result exhibit that the interaction between the Au atom of the AuBN cluster and the π-electrons of the six-membered ring of the guanine is a chemical adsorption in nature. The calculated E_{ads} for this configuration was found to be – 25.3 kcal mol^{-1}, which is much higher (~ 3.5 times) than the values predicted for the two complexes A and B (see Table 1) where the guanine was adsorbed parallel to the surface of the pure BN nanosheet. Moreover, the results suggest that the substitution of a B atom of the BN nanosheet by an Au atom was greatly improved its surface reactivity, thus the Au atom is considered as an active site toward the nucleophilic centers. The estimated length between the guanine molecule and the surface of the cluster is 2.37 Å, which is a bit lower than the values predicted for the configurations A and B.

Also, it is important to note that the adsorption of the guanine over the surface of the AuBN nanosheet by its oxygen atom was also optimized, and the results indicate that the optimized complex from this initial geometry was found identical to that of the complex C. The results show also that the length of the Au-N bond of the AuBN cluster in the complexes formed by its interaction with the guanine molecule was found to be between 2.03 and 2.08 Å, which is a bit lower than that of the isolated AuBN cluster, indicating that the guanine adsorption onto the surface of the AuBN cluster did not significantly alter their structural parameters. The calculations show also that the values of ΔH for the complexes are in the range of – 26.7 to – 42.4 kcal mol^{-1}, and the values of ΔG vary from – 14.0 to – 28.8 kcal mol^{-1}, reflecting that the formation process of the complexes is exothermic and thermodynamically realizable at normal conditions.

A great change in the energies of HOMO and LUMO orbitals (E_H and E_L) was clearly observed (Table 3) for the complexes which were formed after the adsorption guanine over the AuBN cluster. The energies of HOMO and LUMO states of all the studied complexes (C-G) were shifted to the less negative values. For example, the HOMO and LUMO levels shift from – 6.313 and – 3.611 eV in the AuBN cluster to – 5.297 and – 2.870 eV in the complex C, thereby a variation in E_H and E_L of 16 and 20 %, respectively. Based on

the energies of HOMO and LUMO orbitals, the E_g of the complexes were calculated, and the values obtained are listed in Table 3. As it was shown in this table, the electronic properties of the AuBN cluster were largely influenced by the interaction of the guanine molecule onto its surface. As the guanine adsorption over the surface of the AuBN cluster has considerably modified their energies of HOMO and LUMO states, thereby their energy gap (E_g). As an example, the energy gap was decreased from 2.701 eV in the AuBN cluster to 2.364 eV in the complex E, thereby a variation in E_g of 0.337 eV. Based on the Eq. (4), the decrease in E_g of the cluster greatly raised its electrical conductivity, thus it can generate an electrical signal. This result suggests that this cluster could be an appropriate nanosensor for the guanine molecule detection.

The spatial orientations of the HOMO and LUMO orbitals of the cluster and their complexes formed after its interaction with the guanine molecule are depicted in Fig. 7. As one can see from this figure, the HOMO and LUMO states for the AuBN cluster are completely localized on the Au atom. When the guanine molecule is chemisorbed over the surface of the AuBN cluster, the electron density is mostly located on the Au atom of the cluster and around the chemical bond that bind the cluster with the guanine molecule. Also, a low distribution of the electron density was observed onto the guanine molecule. This result suggests a strong interaction between the AuBN cluster and the guanine molecule confirming a chemisorption process in all the studied complexes. This result was also supported by the spin density of the complexes (not shown), which exhibit a large localization of electrons between the Au atom of the AuBN cluster and the guanine, implying a great chemical adsorption between both species. In order to investigate the nature of the formed bonds in the complexes upon the interaction of the guanine with the AuBN cluster, the EDD isosurfaces were calculated for the formed complexes and the results obtained are illustrated in Fig. 8. The results show that the electron density was greatly accumulated around the Au atom of the cluster and the guanine molecule, indicating a great chemical adsorption between both species. This finding was confirmed by the highest obtained E_{ads} values for the complexes, implying a chemisorption process.

In order to determine the quantities of charge transferred between the AuBN cluster and the guanine molecule during the formation of the complexes, AIM charges on each atom in all the considered complexes was calculated and analyzed. The values obtained are summarized in Table 3. As it was reported in this table, a sizable charge was transferred from the guanine molecule to the AuBN cluster in all the studied configurations and the calculated q_{CT} values for the complexes range from 0.152 to 0.727 |e|. The large charge transfer between both species reflects a strong adsorption of the guanine molecule over the surface of the AuBN cluster. The adsorption of the guanine over the AuBN cluster affects also its electric dipole moment. The results indicate that the β_T values of the formed complexes after interaction between the cluster and the guanine were largely augmented, and the calculated values are in the range of 3.201 to 13.941 D. The highest β_T value was obtained for the complex C.

3.3 Adsorption of the guanine molecule over the Nb-BN nanosheet

In this section, we have investigated the interaction of the guanine with the surface of the NbBN cluster in aim to evaluate its electronic sensitivity. In the same way as above, we have placed the guanine molecule on the surface of the NbBN cluster with different orientations in aim to obtain the most stable adsorption configurations. After full optimization, five stable complexes were obtained (H, I, J, K and L configurations), in which their geometries are completely different to those predicted for the AuBN complexes formed from the AuBN cluster (see Figure S1). The interaction distance, energies of the HOMO and LUMO states (E_H, E_L) energy gap (E_g), adsorption energy (E_{ads}) and thermodynamic parameters (ΔH, ΔS and ΔG) of the complexes were summarized in Table 3. As shown from this table, the adsorption guanine onto the surface of the NbBN cluster was carried out without deformation of the molecule and the calculated adsorption energies vary from − 36.7 to − 60.2 kcal mol^{-1}. These obtained values are larger than those computed for the guanine adsorption over the AuBN cluster, except for the K configuration, where E_{ads} was found a bit lower in comparison with that predicted for the complex F (− 38.4 kcal mol^{-1}). This great adsorption between the guanine and the NbBN cluster reflects that the NbBN cluster is more reactive than the AuBN cluster, confirming the above obtained results for the chamical hardness, softness and Fukui function. In the complex H, the guanine adsorption over the surface of the NbBN nanosheet occurs by its oxygen atom with an adsorption energy of − 60.2 kcal mol^{-1}, which is much greater than that found for the other complexes. The calculated length of the Nb-O bond in the formed complex (H) upon chemisorption process is 2.39 Å. Unlike the interaction between the AuBN cluster and the guanine molecule, the charge transfer in this case occurs from the NbBN cluster to the guanine in all the studied complexes, except for the K complex, where a low charge of 0.025 |e| was transferred from the guanine molecule to the NbBN cluster. This configuration corresponds to the lowest E_{ads} value (− 36.7 kcal mol^{-1}) in comparison with the estimated E_{ads} values for the other complexes. The calculated E_{ads} for the I, J and L configurations are − 57.2, − 50.5 and − 42.1 kcal mol^{-1}, respectively, suggesting a great chemisorption between the guanine and the NbBN cluster. The quantity of charge transferred between both species is of 0.682, 0.045, 0.181 and 0.079 |e| for the configurations H, I, J and L, respectively. The interaction distance between the guanine molecule and the surface of the NbBN cluster in the complexes I, J, K and L varies between 2.27 and 2.55 Å (Table 3).

It is interesting to note also that when we have optimized the configuration where the guanine molecule was chemisorbed through its nitrogen atom of $-NH_2$ group, the calculations revealed that the optimized geometry of the complex was found similar to that of the complex K. The results show also that the calculated distance of the Nb-N bond in the NbBN cluster after its interaction with the guanine molecule is in the range of 2.00 to 2.06 Å, which is remained almost unchanged with respect to the value calculated for the isolated NbBN nanosheet, implying that the strong interaction of the guanine over the surface of the NbBN cluster has not modified their structural parameters. The results indicate also that the calculated values of ΔH and ΔG for the complexation process are negative, indicating that the complexation process of the guanine over the surface of the NbBN cluster was found to be exothermic and thermodynamically feasible at ambient temperature (T = 298.15 K) and pressure (1 atm).

The change in the energies of frontier molecular orbitals (FMO) for the complexes which are formed from the interaction of the guanine with the NbBN cluster was clearly observed (Table 3). As it was reported in Table 3, the energies of HOMO orbitals for the configurations J, K and L are shifted to the more negative values, while for the configurations H and I, the values of HOMO orbitals are shifted to the less negative values. On the other hand, the energies of LUMO orbitals of all the studied complexes were shifted to the less negative values, except for the complex L where its energy of LUMO level remains almost unchanged. As an example, the HOMO level shifts from – 3.540 in NbBN cluster to – 4.146 eV in complex K, whereas the LUMO level shifts from – 2.045 to – 1.569 eV. Based on the energies of HOMO and LUMO states, the energy gaps (E_g) of these complexes are calculated, and the values obtained are reported in Table 3. From this table, it was found that the guanine adsorption over the surface of the NbBN cluster was sharply affected their electronic properties. In contrast to the results obtained for the AuBN cluster, the energy gap of the NbBN nanosheet was largely increased when the guanine molecule adsorbs on its surface. The variation in energy gap (ΔE_g) for the configurations J, K and L is 80.9 %, 72.4 % and 45.5 %, respectively, whereas for the configurations H and I, the calculated ΔE_g is mall (ΔE_g < 13 %). This result indicates that the Nb-doped BN nanosheet is very sensitive to the adsorption of guanine onto its surface. Accordingly to the Eq. (4), the electrical conductivity of the NbBN cluster was sharply reduced when the guanine molecule was strongly chemisorbed over its surface, thereby the NbBN cluster can be considered as not suitable nanosensor for the detection of the guanine molecule.

The spatial orientations of the HOMO and LUMO levels of the NbBN cluster and their interaction with the guanine molecule are depicted in Figure S2. From this figure, the results indicate that the HOMO and LUMO orbitals are mostly localized on the Nb atom for the NbBN nanosheet. When the guanine molecule was chemisorbed over the NbBN cluster, the density of HOMO remains unchanged, and the electron density is completely located around the Nb atom of the cluster. While the LUMO orbitals are mainly localized over the Nb atom of the cluster and the guanine molecule. This result suggests a strong chemisorption process between the Nb atom of the NbBN cluster and the guanine molecule in all the formed complexes. This finding has also been confirmed by the spin density which was calculated for the complexes (not shown), which exhibits a large localization of electrons between the Nb atom of the cluster and the guanine molecule.

In order to investigate the nature of the formed bonds in the complexes upon interaction of the guanine with the NbBN cluster, the EDD isosurfaces were calculated and the results predicted are shown in Figure S3. For example, in the configuration H, the EDD isosurface reveal that the electron density is mainly accumulated around the Nb-N bond, reflecting a great chemical adsorption between the guanine molecule and the Nb atom of the NbBN cluster (chemisorption process). Identical results were obtained for the other complexes (I, J, K and L), where the electron density accumulation has also been mostly observed between the surface of the NbBN cluster and the guanine molecule, suggesting a chemisorption process. The results exhibit also that the electric dipole moment (β_T) of these complexes was augmented after the adsorption process (Table 3), and the highest β_T value was predicted for the complex H (15.563 D), where

the chemisorption of the guanine over the surface of the NbBN cluster was carried out by its oxygen atom.

3.4 Recovery time

A shorter recovery time can be obtained if the interaction between the cluster and the guanine molecule is not strong. The great adsorption makes the desorption of the molecule from the cluster surface very hard, which leads to long recovery time. Therefore, the cluster does not become a suitable nanomaterial for nanosensor applications. In other words, the strong adsorption between the molecule and the cluster reduces the efficiency and significance of the cluster as a nanosensing. Using an attempt frequency of 10^{14} s^{-1} to desorbs the guanine molecule which is attached to the surface of the AuBN clusters, the recovery time at 540 K was estimated to be 27.6 s which is considered as a short time for the desorption of the guanine from the cluster surface. Therefore, the AuBN cluster can be viewed as a good nanosensor for the guanine molecule with a short recovery time. Also, it is interesting to say that the recovery time could be greatly reduced when the temperature was raised. So, the higher temperatures facilitate the desorption process of the guanine molecule through the surface of the AuBN cluster. Unfortunately, there is no experimental or theoretical results to compare with our theoretical values obtained in this work. Therefore, this theoretical study could be a window for experimenters to draw attention to the AuBN cluster as a nanosensor for the guanine molecule or other drug molecules.

4. Conclusions

In the present work, the stability and electronic properties of the pristine, Nb- and Au-doped BN nanosheet were investigated using DFT calculations with the B3LYP-D3 level of theorey. The interaction of the guanine molecule with the surface of these clusters have also been examined. The results show that the HOMO-LUMO energy gap of the BN nanosheet has been greatly decreased upon its doping with Nb and Au atoms, suggesting a great enhancement in its reactivity. This finding was supported by the calculated values of the hardness (softness) for the AuBN and NbBN clusters which are found to be lower (greater) than that obtained for the pure BN nanosheet, reflecting a increase in their surface reactivity. Moreover, the condensed Fukui function indicates that the Nb and Au atoms in the clusters are considered as the most favorable adsorption sites for nucleophilic attack. The calculations show also that the interaction between the BN nanosheet and the guanine is weak (physical adsorption), and the calculated adsorption energies are – 15.2 and – 14.9 kcal mol^{-1} for the complexes A and B, respectively. The variation in E_g of the BN nanosheet after its interaction with the guanine molecule was found to be 14.9 and 13.2 % in the A and B states, respectively, implying a low sensitivity of this cluster towards the guanine molecule. The interaction of the guanine with the NbBN and AuBN clusters has also been investigated. The results indicate a strong adsorption of the guanine molecule over the surface of the NbBN cluster with adsorption energies which vary between – 36.7 and – 60.2 kcal mol^{-1}, indicating a great chemisorption process. The energy gap of the NbBN cluster was greatly raised when the guanine molecule was chemisorbed on its surface, thereby its electric conductivity was sharply reduced, thereby this cluster could not be a good nanosensor for the detection of the guanine molecule. The guanine adsorption onto

the surface of the AuBN cluster is considered as a chemical adsorption with adsorption energies ranging from – 24.2 to – 38.4 kcal mol^{-1}, which are lower in comparison with those obtained for the guanine adsorption onto the surface of the NbBN cluster. Contrary to the NbBN cluster, the energy gap of the AuBN cluster has been reduced upon its interaction with the guanine molecule, which increases its electrical conductivity, thus an electrical signal can be generated. So, the AuBN cluster could be employed as an appropriate nanosensor for the guanine molecule detection. Moreover, the calculations show that the recovery time of the guanine molecule which was attached to the surface of the AuBN cluster is found to be 27.6 s, which is considered as a very short recovery time. This suggests that the desorption of the guanine from the cluster surface occurs easily with a short recovery time. The AIM charges analysis reveals that the charge is transferred from the NbBN cluster to the guanine molecule (except for the configuration K), and the calculated values predicted are in the range of 0.025 to 0.682 |e|. On the contrary, in the complexes formed between the AuBN cluster and the guanine, the charge transfer occurs from the molecule to the cluster, and the amounts of charge transferred between both species varies from 0.152 to 0.727 |e|. The calculations show also that the dipole moments of the clusters (BN, NbBN and AuBN) were increased after their interaction with the guanine molecule.

Declarations

Funding

No funding was received for conducting this work.

Data availability

Data can be obtained through the corresponding author from email.

Code availability

Not applicable

Compliance with ethical standards

Conflict of interest: The authors declare that they have no conflict of interest.

References

[1] Schmid G (1992) Large clusters and colloids. Metals in the embryonic State, Chem. Rev. 92:1709-1727.

[2] Mori K, Miyawaki K, Yamashita H (2016) Ru and Ru-Ni nanoparticles on TiO support as extremely active catalysts for hydrogen production from ammonia borane, ACS Catalysis. 6:3128-3135.

[3] Mokrane T, Boudjahem A, Bettahar M (2016) Benzene hydrogenation over alumina-supported nickel nanoparticles prepared by polyol method, RSC Advances. 6:59858-59864.

[4] Boudjahem A, Mokrane T, Redjel A, Bettahar M (2010) Silica supported nanopalladium prepared by hydrazine reduction, C. R. Chimie. 13:1433-1439.

[5] Liu A, Xu Y, Qiu X, Huang C, Liu M (2019) Chemoselective hydrogenation of nitrobenzenes activated with tuned Au/h-BN, J. Catal. 370:55-60.

[6] Boudjahem A, Bettahar M (2017) Effect of oxidative pre-treatment on hydrogen spillover for a Ni/SiO_2 catalyst, J. Mol. Catal. A. 24:190-197.

[7] Redjel A, Boudjahem A, Bettahar M (2018) Effect of palladium precursor and preparation method on the catalytic performance of Pd/SiO_2 catalysts for benzene hydrogenation, Particul. Sci. Eng. 36:710-715.

[8] Chen N, Zhu Z, Su T, Liao W, Deng C, Ren W, Zhao Y, Lu H (2020) Catalytic hydrogenolysis of hydroxymethylfurfural to highly selective 2,5-dimethylfuran over FeCoNi/h-BN catalyst, Chem. Engin. J. 381:122755.

[9] Boudjahem A, Monteverdi S, Mercy M, Bettahar M, (2004) Nanonickel particles supported on silica. Morphology effects on their surface and hydrogenating properties, Catal. Lett. 97:177–183.

[10] Boudjahem A, Redjel A, Mokrane T (2012) Preparation, characterization and performance of Pd/SiO_2 catalyst for benzene catalytic hydrogenation, J. Ind. Chem. Eng. 18:303-308.

[11] Kon K, Onodera W, Toyao T, Shimizu K (2016) Supported rhenium nanoparticle catalysts for acceptoless dehydrogenation of alcohols: Structure-activity relationship and mechanistic studies. Catal. Sci. Technol. 6:5864-5870.

[12] Shen J, Yang L, Hu K, Luo W, Cheng G (2015) Rh nanoparticles on graphene as efficient catalyst for hydrolytic dehydrogenation of amine boranes for chemical hydrogen storage, Int. J. Hydrogen. Energy. 40:1062-1070.

[13] Wang J, Zhang X, Wang Z, Wang L, Zhang Y (2012) Rhodium-nickel nanoparticles grown on graphene as highly efficient catalyst for complete decomposition of hydrous hydrazine at room temperature for chemical hydrogen storage, Energy. Environ. Sci. 5:6885-6888.

[14] Dong L, Sanganna Gari R R, Li Z, Craig M, Hou S (2010) Graphene-supported platinium and platinium-ruthenium nanoparticles with high electrocatalytic activity for methanol and ethanol oxidation, Carbon. 48:781-787.

[15] Qiu X, Wu X, Wu Y, Liu Q, Huang C (2016) The release hydrogen from ammounia borane over copper/hexagonal boron nitride composites, RSC Advances. 6:106211–106217.

[16] Shen H, Duan C, Guo J, Zhao N, Xu J (2015) Facile in situ synthesis of silver nanoparticles on boron nitride nanosheets with enhanced catalytic performance, J. Mater. Chem. 3:16663–16669.

[17] Goyal A, Aggarwal D, Kapoor S, Goel N, Singhal S, Shukla J (2020) A comprehensive experimental and theoretical study on BN nanosheets for the adsorption of pharmaceutical drugs, New. J. Chem. 44:3985-3997.

[18] Yang H, Gu S, Li J, Jin L, Xie X, Luo L, Xiao J, Li J, Li C, Chen Y (2020) Synthesis of boron carbonitride nanosheets using for delivering paclitaxel and their antitumor activity, Colloid. Surf. B. in press:111479.

[19] Zhang Y, Guo R, Wang D, Sun X, Xu Z (2019) Pd nanoparticle-decorated hydroxy boron nitride nanosheets as a novel drug carrier for chemo-photothermal therapy, Colloid. Surf. B. 176:300-308.

[20] Du M, Liu Q, Huang C, Qiu X (2017) One-step synthesis of magnetically recyclable Co@BN core-sheel nanocatalysts for catalytic reduction of nitroarenes, RSC Advances. 7:35459-35459.

[21] Huang C, Ye W, Liu Q, Qiu X (2014) Dispersed Cu_2O octahedrons on h-BN nanosheets for p-nitrophenol reduction, ACS Appl. Mater. Interfaces. 6:14469–14476.

[22] Fu Q, Meng Y, Fang Z, Hu Q, Xu L, Gao W, Huang X, Xue Q, Sun Y, Lu F (2017) Boron nitride nanosheet-anchored Pd-Fe core-shell nanoparticles as highly efficient catalysts for Suzuki-Miyaura coupling reactions, ACS Appl. Mater. Interfaces. 9:2469–2476.

[23] Huang C, Chen C, Ye X, Ye W, Hu J, Xu C, Qiu X (2013) Stable colloidal boron nitride nanosheet dispersion and its potential application in catalysis, J. Mater. Chem. A 1:12192.

[24] Yang XJ, Li LL, Sang WL, Zhao JL, Wang XX, Yu C, Zhang XH, Tang CC (2017) Boron nitride supported Ni nanoparticles as catalysts for hydrogen generation from hydrolysis of ammounia borane, J. Alloy. Compound. 693:642-649.

[25] Behmagham F, Vessally E, Massoumi B, Hosseinian A, Edjlali L (2016) A computational study on the SO_2 adsorption by the pristine, Al, and Si doped BN nanosheets, Superllatices. Microstructures. 100:350-357.

[26] Zhao P, Su Y, Zhang Y, Li SJ, Chen G (2011) CO catalytic oxidation on iron-embedded hexagonal boron nitride sheet, Chem. Phys. Lett. 515:159-161.

[27] Esrafili MD (2018) NO reduction by CO molecule over Si-doped boron nitride nanosheet: A dispersion-corrected DFT study. Chem. Phys. Lett. 695:131-137.

[28] Lee JH, Choi YK, Kim HJ, Scheicher R, Cho JH (2013) Physisorption of DNA nucleobaseson h-BN and graphene: vdW-corrected DFT calculations. J. Phys. Chem. A 117:13435-13441.

[29] Lin Q, Zou X, Zhou G, Liu R, Wu J, Li J, Duan W (2011) Adsorption of DNA/RNA nucleobases on hexagonal boron nitride sheet: an ab initio study. Phys. Chem. Chem. Phys. 13:12225-12230.

[30] Singla P, Riyaz M, Singhal S, Goel N (2016) Theoretical study of adsorption of amino acids on graphene and BN sheet in gas and aqueous phase including empirical DFT dispersion correction. Phys. Chem. Chem. Phys. 18:5597-5604.

[31] Frisch MJ, Trucks GW, Schlegel HB, Scuseria GE, Robb MA, Cheeseman JR, Scalmani G, Barone V, Mennucci B, Petersson GA, Nakatsuji H, Caricato M, Li X, Hratchian HP, Izmaylov AF, Bloino J, Zheng G, Sonnenberg JL, Hada M, Ehara M, Toyota K, Fukuda R, Hasegawa J, Ishida M, Nakajima T, Honda Y, Kitao O, Nakai H, Vreven T, Jr JA, Montgomery JE, Peralta F, Ogliaro M, Bearpark JJ, Heyd E, Brothers KN, Kudin VN, Staroverov T, Keith R, Kobayashi J, Normand K, Raghavachari A, Rendell JC, Burant SS, Iyengar J, Tomasi M, Cossi N, Rega JM, Millam M, Klene JE, Knox JB, Cross V, Bakken C, Adamo J, Jaramillo R, Gomperts RE, Stratmann O, Yazyev AJ, Austin R, Cammi C, Pomelli JW, Ochterski RL, Martin K, Morokuma VG, Zakrzewski GA, Voth P, Salvador JJ, Dannenberg S, Dapprich AD, Daniels O, Farkas JB, Foresman JV, Ortiz J, Cioslowski DJ (2013) Fox, Gaussian 09, Revision D.01. Gaussian, Inc., Wallingford

[32] Becke AD (1988) Density-functional exchange-energy approximation with correct asymptotic behavior. Phys. Rev. A 38:3098–3100.

[33] Becke AD (1993) Density-functional thermochemistry. III. The role of exact exchange. J. Chem. Phys. 98:5648-5652.

[34] Lee C, Yang W, Parr R (1988) LYP correlation functional, Phys. Rev. B. 37:785.

[35] Charkin OP, Klimenko NM, Charkin DO (2019) DFT modeling of successive hydrogenated subnano-size aluminum clusters, Chem. Phys. 522:112-122.

[36] Rad SA, Esfahanian M, Maleki S, Gharati G (2016) Application of carbon nanostructures toward SO_2 and SO3 adsorption: A comparison between pristine graphene and N-doped graphene by DFT calculations. J. Sulf. Chem. 37:176–188.

[37] Hay PJ, Wadt WR (1985) Ab initio effective core potentials for molecular calculations. Potentials for K to Au including the outermost core orbitals. J. Chem. Phys. 82:299-310.

[38] Krishnan R, Binkley JS, Seeger R, Pople JA (1980) Self-consistent molecular orbital methods. XX. A basis set for correlated wave functions. J. Chem. Phys 72:650-654.

[39] Soltani A, Boudjahem A (2014) Stabilities, electronic and magneticproperties of small Rh_n (n=2–12) clusters : A DFT approach. Comput. Theor. Chem. 1047:6–14.

[40] Padash R, Nasrabadi M, Rad AS, Nasab AS (2018) Jesionowski T., H. Ehrlich, A Comparative Computational Investigation of Phosgene Adsorption on (XY)12 (X = Al, B and Y = N, P) Nanoclusters:

DFT Investigations. J. Clust. Sci. 30:203–218.

[41] Karaman A, Boudjahem A, Boulbazine M, Gueid A (2020) Stability and electronic properties of Ir_nV (n = 2–10) nanoclusters and their reactivity toward N_2H_4 molecule. Struct. Chem. 31:203-214.

[42] Boulbazine M, Boudjahem A, Chaguetmi S, Karaman A (2020) Stability and electronic properties of Rh-doped ruthenium clusters and their interaction with NH_3 molecule. Mol. Phys. 118:e1643511.

[43] Chermette H (1999) Chemical reactivity indexes in density functional theory, J. Comput. Chem. 20:129-154.

[44] Ersanm F, Gokoglu G, Akturk E (2014) Bimetallic two-dimensional PtAg coverage on h-BN substrate: First-principles calculations. Appl. Surf. Sci. 303:306-311.

[45] Xu D, Liu YJ, Zhao JX, Cai QH, Wang XZ (2014) Theoeretical study of the deposition of Pt clusters on defective hexagonal boron nitride (h-BN) sheets : Morphologies, electronic structures, and interactions with O, J. Phys. Chem. C 118:8868-8876.

[46] Solozhenko VL, Lazarenko AG, Petitet JP, Kanaev AV (2001) Band gap energy of graphite-like hexagonal boron nitride, J . Phys. Chem. Solids. 62:1331-1334.

[47] Bouderbala W, Boudjahem A, Soltani A (2014) Geometries, stabilities, electronic and magnetic properties of small Pd_nIr (n = 1–8) clusters from first-principles calculations, Mol. Phys. 112:1789–1798.

[48] Soltani A, Boudjahem A, Bettahar M, (2016) Electronic and magnetic properties of small Rh_nCa (n = 1-9) clusters: A DFT study, Int. J. Quantum. Chem. 5:346-356.

[49] Pansini FN, Campos M, Neto AC, Sergio CS (2020) Theoretical study of the electronic structure and electrical properties of Al-doped niobium clusters, Chem. Phys. 535:110778.

[50] Cheng S, Sun X, Zhao L, Chen J (2019) The interaction of guanine nucleobase with B_{40} borospherene. Eur. Phys. J. D 73:88.

Figures

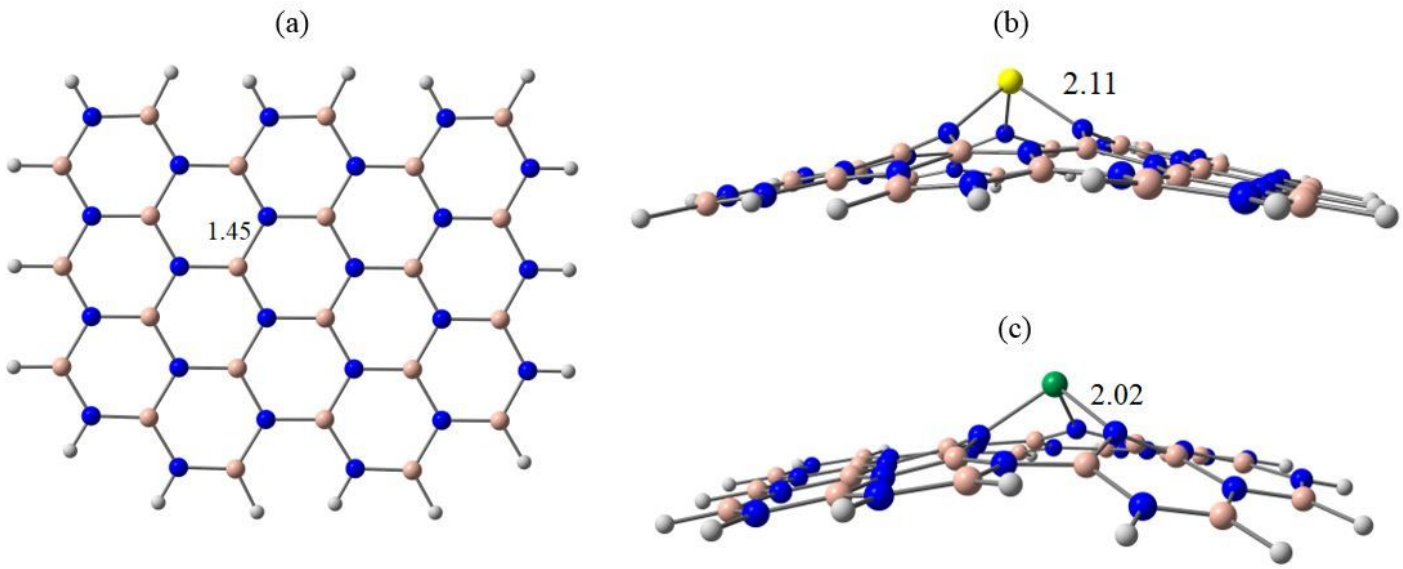

Figure 1

The optimized geometries of the (a) pristine, (b) Au- and (c) Nb-doped BN nanosheets.

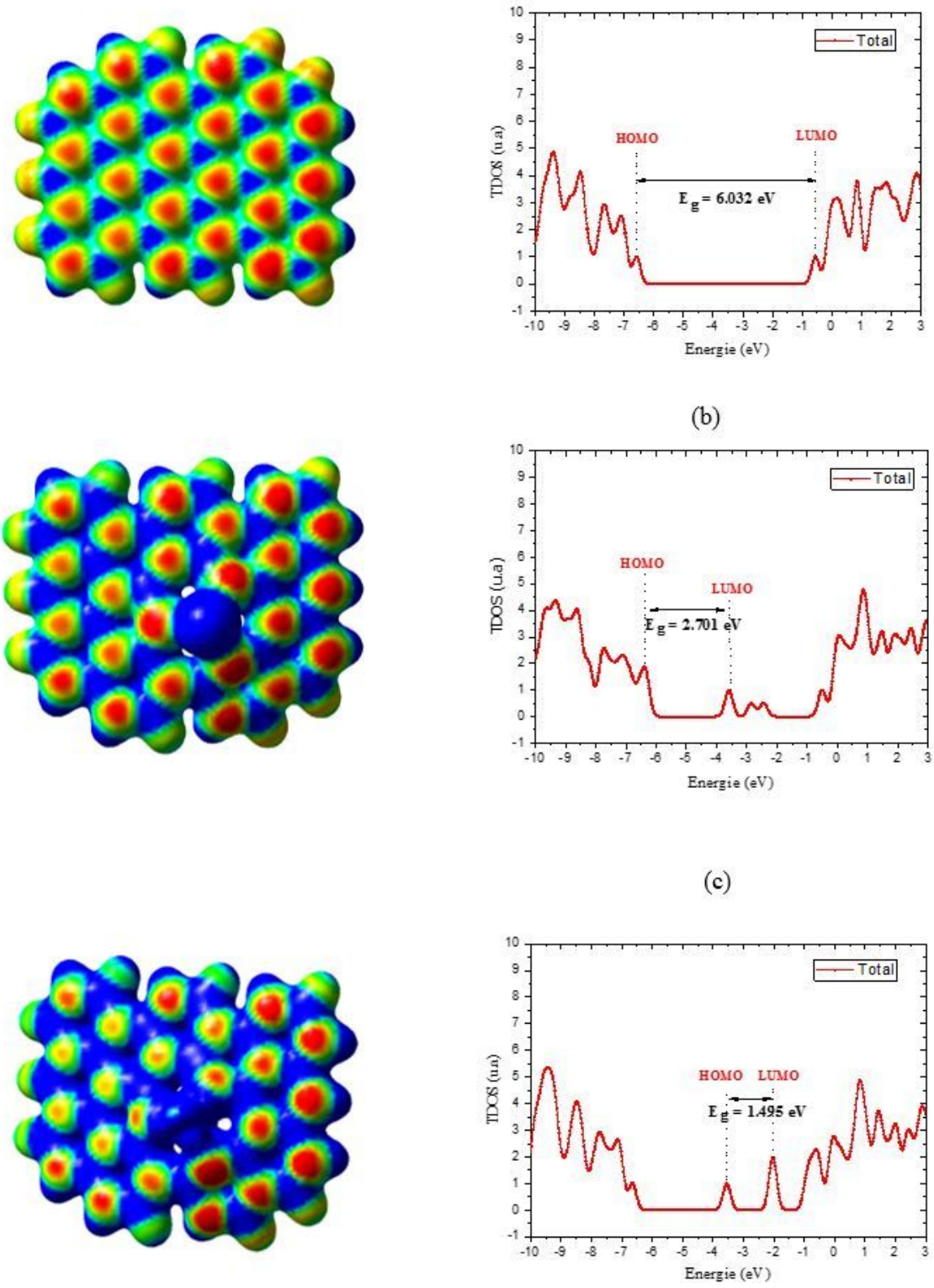

Figure 2

Molecular electrostatic potential maps (MEP) and density of states (DOS) of the (a) pristine, (b) Au-and (c) Nb-doped BN nanosheets.

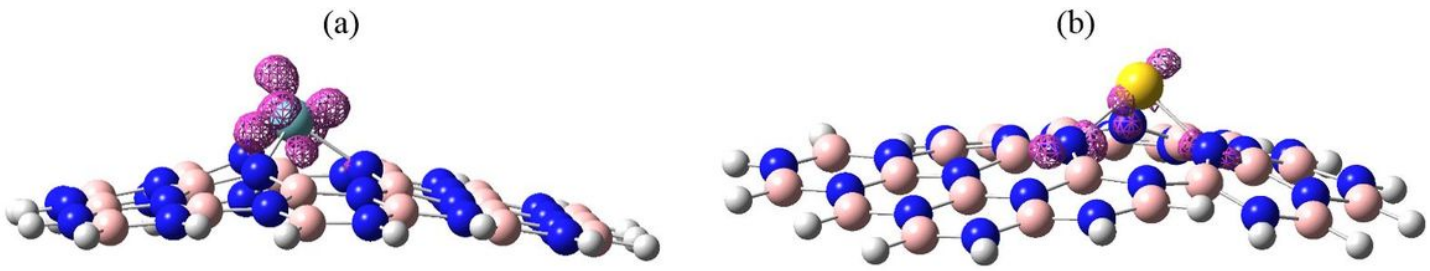

Figure 3

The isosurface of f + of the Nb- and Au-doped BN nanosheets.

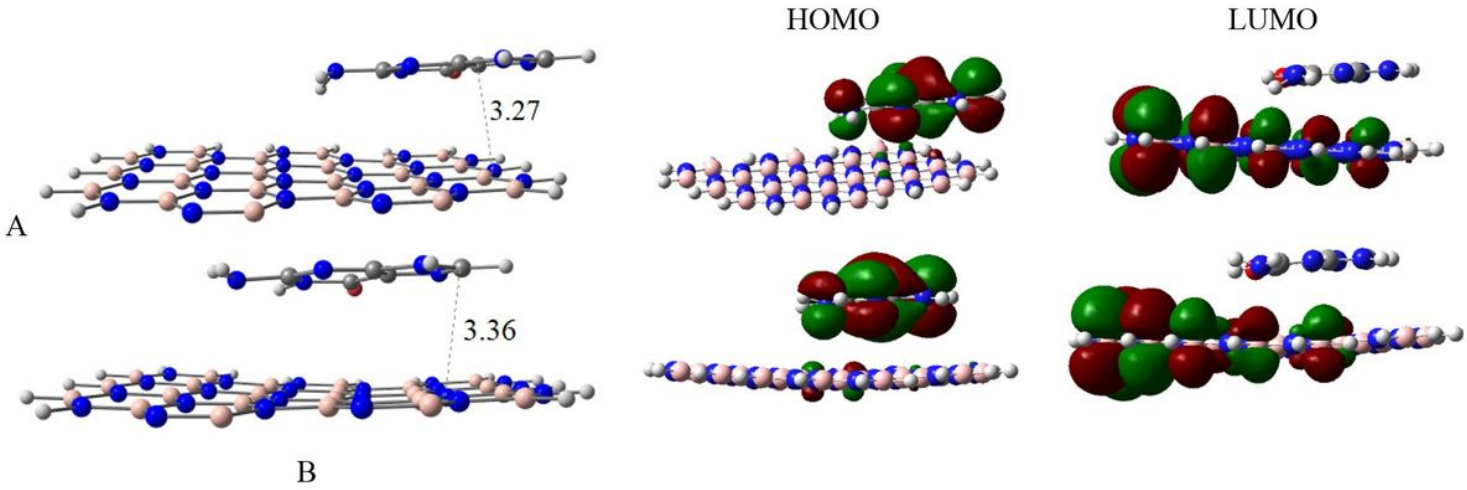

Figure 4

The optimized geometries of the complexes formed by the guanine adsorption over the surface of the BN nanosheet (A and B complexes) and their HOMO and LUMO orbitals.

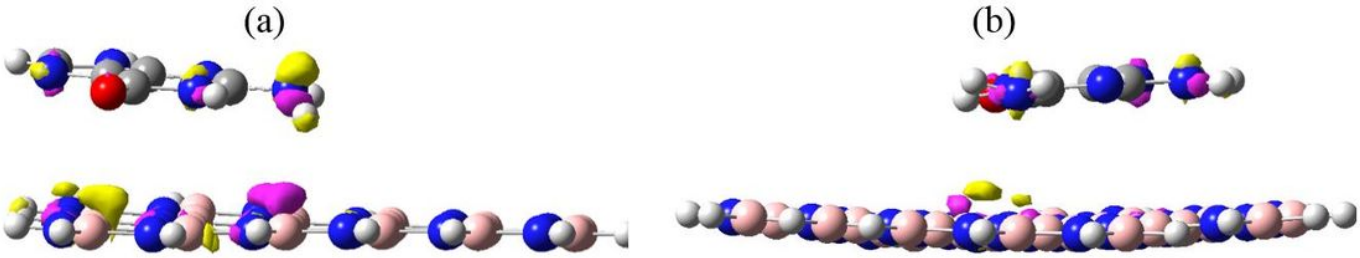

Figure 5

The electron density difference (EDD) isosurfaces for the complexes A and B. The pink and yellow represent the electron density gain and loss regions, respectively.

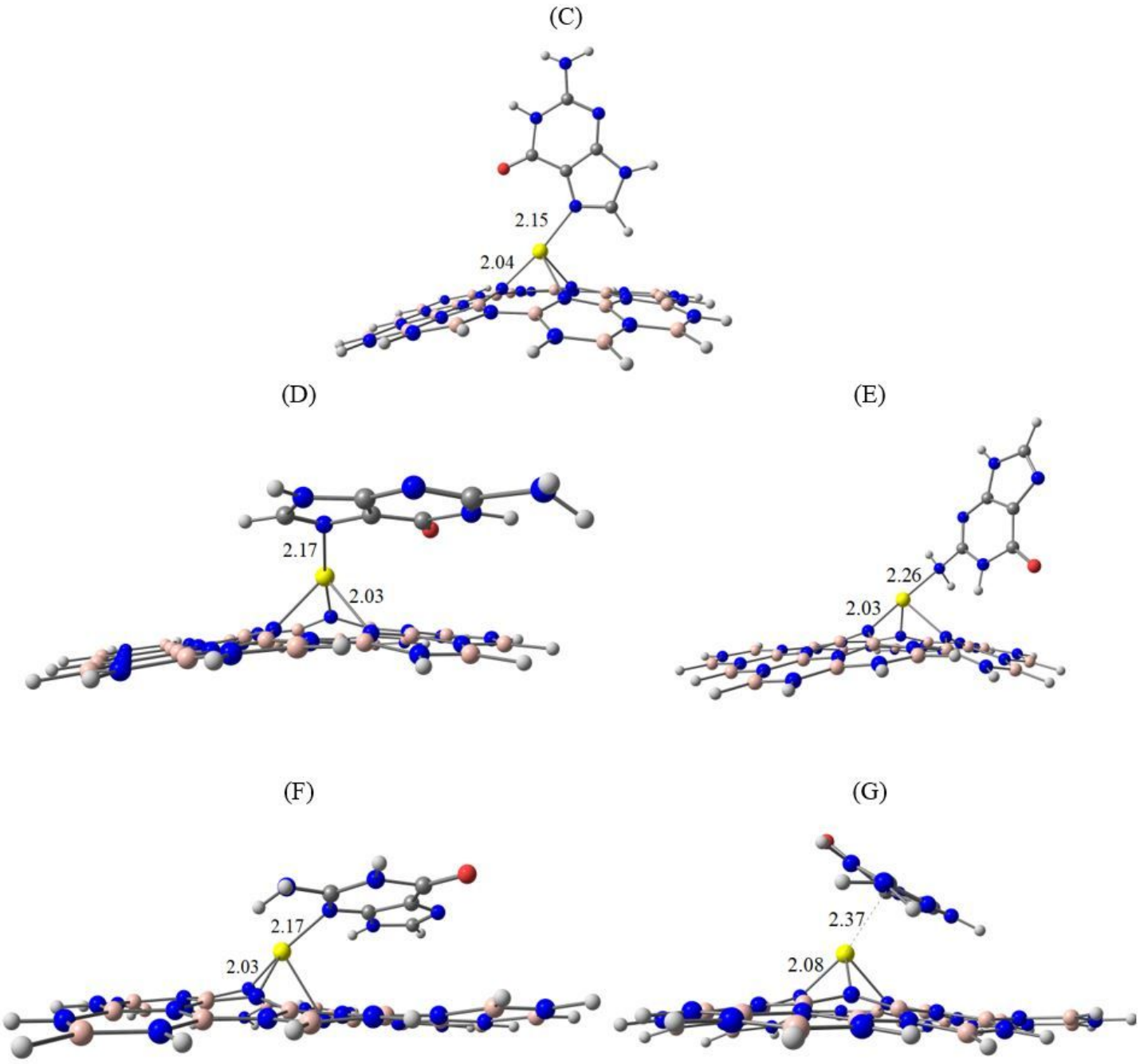

Figure 6

The most stable complexes obtained upon interaction of the guanine molecule with the surface of the AuBN cluster (C, D, E, F and G).

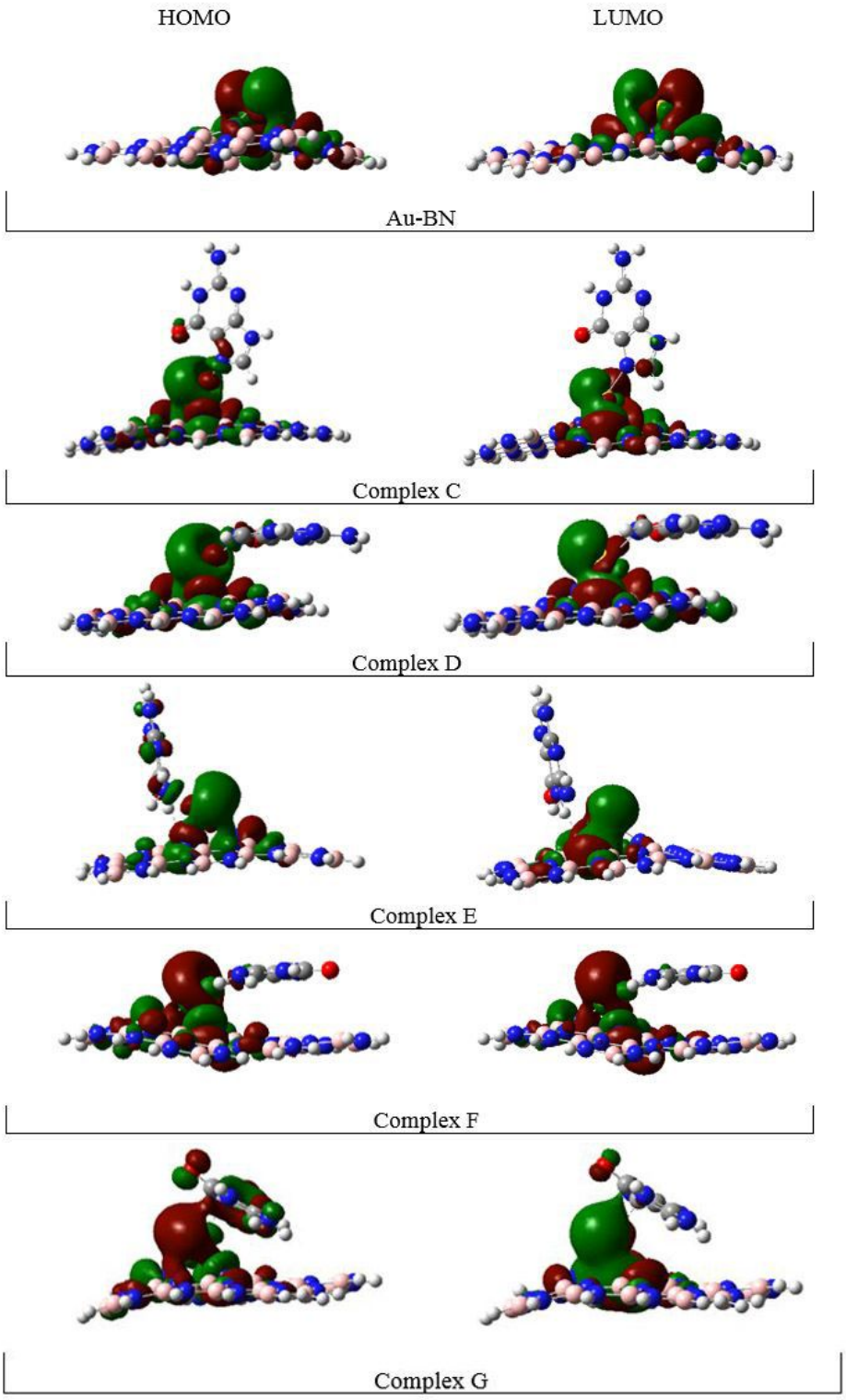

Figure 7

Frontier molecular orbitals (FMO) plots of the Au-doped BN nanosheet and their formed complexes upon interaction with the guanine molecule (C, D, E, F and G).

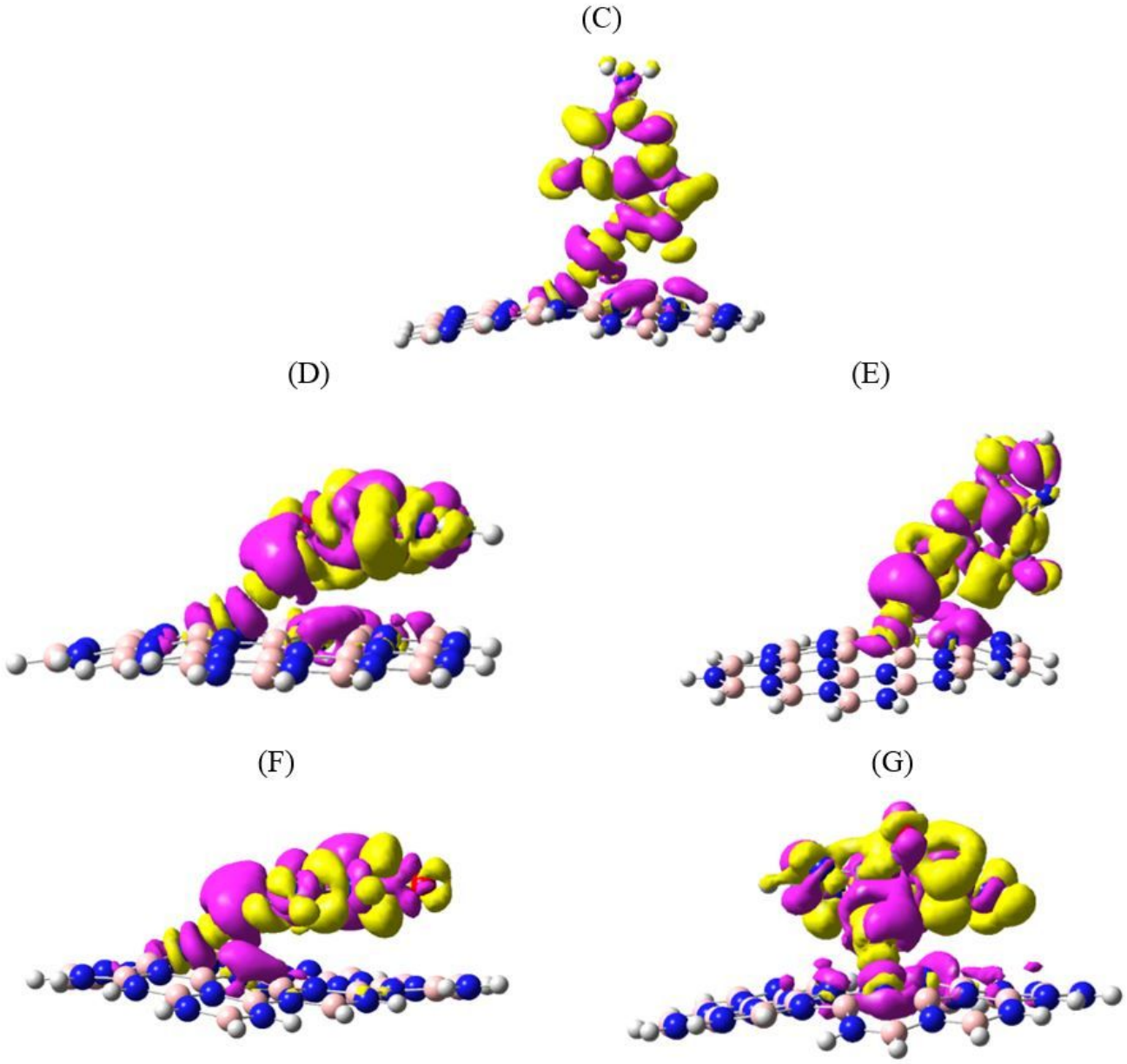

Figure 8

The electron density difference (EDD) isosurfaces for the complexes C, D, E, F and G.

Supplementary Files

This is a list of supplementary files associated with this preprint. Click to download.

- MBNSUPPLFigstablesSTRUCHEMZZZ2021bon.docx